

Urban Landscape Recovery and LULC Analysis: A Deep Learning Approach to Post-Extreme Rainfall Impacts in Dubai

Xin Hong¹

¹ Department of Environmental Sciences and Sustainability, College of Natural and Health Sciences, Zayed University, Abu Dhabi, the United Arab Emirates – xin.hong@zu.ac.ae

Keywords: LULC classification, U-Net, PlanetScope, urban resilience assessment, extreme rainfall

Abstract

From April 14 to 18, 2024, the United Arab Emirates (UAE) experienced its heaviest rainfall in 75 years, resulting in widespread flooding across multiple emirates, including Dubai. This study utilizes high-resolution PlanetScope imagery and a U-Net deep learning model to assess the flood impact and analyze post-rainfall recovery patterns in Dubai's urban landscape. By integrating Sentinel-2-derived land use and land cover (LULC) data to refine the training dataset, a high-accuracy U-Net model was developed through transfer learning that effectively classified pre- and post-rainfall LULC. Post-rainfall LULC change detections indicate that 23.8 km² of land was flooded, which is equivalent to about 10 times the area of Downtown Dubai. Bare ground (66% of the flooded land) and built area (32% of the flooded land) were the most affected, while vegetation (2% of the flooded land) presented greater flood resilience. Post-event monitoring revealed that 95% of flooded areas remained submerged after three days and 37% were still underwater even ten days post-event. These findings highlight the prolonged impact of extreme rainfall on urban infrastructure in an arid environment. This study contributes to remote sensing-based flood impact assessment by leveraging high-resolution PlanetScope imagery and deep learning techniques. It demonstrates the effectiveness of transfer learning in improving LULC classification, particularly for minority classes such as small-patch vegetation. The results provide critical insights into urban flood recovery dynamics and offer valuable information for disaster management, flood resilience planning, and future urban adaptation strategies.

1. Introduction

The Gulf region experienced its most intense rainfall event in 75 years between April 14 and 18, 2024, severely affecting United Arab Emirates, Bahrain, Qatar, Saudi Arabia and Oman. In Dubai, the downpour began late on April 15th, intensified the next morning, continued throughout April 16th, and officially concluded in April 17th (McCabe, 2024). The city recorded approximately 250 mm of precipitation within 24 hours—more than twice its annual average rainfall of 97 mm (Oxford Analytica, 2024; Rannard, 2024; UAEGOV, 2024). This unexpected deluge triggered flash floods that caused significant and immediate socio-economic disruptions. Major highways in Dubai were submerged, halting transportation. Schools were closed, and many residents transitioned to remote work. Households suffered from prolonged outages of water and power supplies (Alawlaqi, 2024; Ahmad et al., 2024; JBA Response, 2024; The National, 2024). Strong winds also led to over 1,000 flight cancellations at Dubai International Airport (Cornish and Georgiadis, 2024). The flooding underscored the vulnerabilities of urban infrastructure in the face of extreme weather events and highlighted the widespread damage caused by flash floods, emphasizing the need to monitor the destruction of urban infrastructure and landscapes. Given the scale of the disaster, precise and timely flood mapping and land use and land cover (LULC) change tracking are critical for understanding recovery dynamics and supporting disaster management efforts.

Remote sensing has been widely used to map flooding, assess post-disaster management, and urban resilience monitoring. Open-source LULC classification data derived from Sentinel-2 MSI imagery at 10 m resolution has proven effective for large-scale LULC change detections (Lombana and Martínez-Graña, 2022). However, finer-scale analysis in urban landscape within arid environments, especially for small-scale features like vegetation, requires higher spatial resolution imagery. PlanetScope imagery, with 3 m resolution and daily revisit characteristics, provides such detailed insights but has been less explored in LULC classification and flood mapping (Basheer et al., 2024; Chanda and Hossain, 2024). As of the time this paper

was written, PlanetScope offers 3,000 km² a month of free imagery for users affiliated with an educational institution for education and research purposes (Planet, 2025). This suggests that PlanetScope imagery is freely available with extensive coverage for a large academic community. The integration of Sentinel-2 derived LULC data and PlanetScope imagery with deep learning models offers an opportunity to improve classification process and monitor post-disaster recovery at finer spatial and temporal scales.

This study used a U-Net convolutional natural network (CNN) model proposal by Ronneberger et al. (2015) to classify LULC before and after the April 2024 heavy rainfall in Dubai. Subsequently, the flooded areas and LULC recovery dynamics were detected using change detection method in a GIS environment. The main objectives were: (1) to classify LULC using a U-net architecture on PlanetScope imagery for pre- and post-event dates; and (2) to analyze the spatial and temporal recovery dynamics across different LULC classes. This work contributes to advancing methodologies for flood impact assessment and urban resilience monitoring.

2. Methods

2.1 Study Area and Datasets

The study area Dubai City was delineated based on the boundary shapefile provided by ESRI (2024) and modified to include more coastal water areas and islands. The total area covers approximately 1,534 km² (Figure 1). The workflow included three main steps: (1) training sample generation, (2) U-Net model training and LULC classification, and (3) flooded areas identification and temporal analysis of landscape recovery after the rainfall.



Figure 1. The boundary of study area, Dubai city (confined by red line).

PlanetScope imagery (Planet Labs PBC, 2024) with eight multispectral bands at 3 m resolution, captured on the pre-rainfall date of April 14 and post-rainfall dates of April 18, 20, 25, 26, and 27, 2024, was used to derive the LULC classifications. The open-access 2023 LULC classification data at 10 m resolution derived from Sentinel-2 by Karra et al. (2021) was used as the reference dataset for initiating data annotation. The reference data was refined through manual corrections by cross-referencing it with the April 14 PlanetScope scene to align with the on-ground conditions prior to the rainfall. This combined usage of the Sentinel-2 LULC data and the April 14 PlanetScope scene in data annotation improved the efficiency of generating large sample datasets and ensured data accuracy for the CNN model training. The sample dataset contains four LULC categories: water, vegetation, built area, and bare ground. A total of 1,188 annotated image slices of 256×256 pixels with a stride of 128×128 pixels were generated and used for training the CNN model.

2.2 U-net Training for LULC Classification

A U-Net model was trained in two stages for LULC classification using Train Deep Learning Model tool in ArcGIS Pro 3.4. (Redlands, 2025) The initial, baseline U-net model was trained with a ResNet34 backbone at a learning rate of 0.0001, using the Adam optimizer for 20 epochs. Given class imbalance in the dataset, where vegetation samples appeared as smaller patches and in lower quantities compared to other classes, class balancing was enabled with a class weight of 2.0 for vegetation. To improve segmentation accuracy, particularly for minority classes, the focal loss with a dice loss fraction of 0.5 was used as the loss function. The batch size was 32, and the dataset was split into 80% for training and 20% for validation. Validation loss was monitored to guide early stopping and prevent overfitting.

The initial, trained U-net model demonstrated relatively low recall and F1 scores for vegetation class (Table 1). To address this, the model was employed as a pre-trained model to train the U-Net architecture again through transfer learning. During the transfer learning process, the learning rate was reduced to 0.00005, and augmentation strategies were refined in zoom, brightness, contrast, and cropping to improve segmentation results. This approach significantly improved classification performance, and the final model was applied to classify PlanetScope imagery for pre-rainfall (April 14) and post-rainfall dates (April 18, 20, 25, 26, and 27).

2.3 Post-Rainfall Recovery Analysis

The categorical LULC changes between the April 14 LULC classification data (pre-rainfall) and the April 18 LULC classification data (the day after rainfall) were mapped and summarized to reveal the flooded areas using the Change Detection Wizard tool in ArcGIS Pro 3.4. The change detection focused specifically on transitions from vegetation, built areas, and bare ground to water, identifying the extent of flooded regions. Subsequently, the recovery of flooded areas in the post-rainfall dates of April 20, 25, 26, and 27 were monitored, as revealed by the inter-class change dynamics among LULC categories.

3. Results and Discussion

3.1 Classification Metrics from U-net

The initial U-Net model's training and validation loss graph indicates consistent learning behavior, with the validation loss decreasing over epochs and stabilizing towards the later stages (Figure 2). Key metrics for the model indicate good classification performance across water, built area, and bare ground classes, with precision, recall, and F1-scores showing reliable predictions. For example, the water class demonstrated high precision (0.9581) and recall (0.9905), leading to a high F1-score of 0.9740. However, vegetation class performance lagged behind, with low values of recall and recall F1-score, highlighting a need for improvement (Table 1).

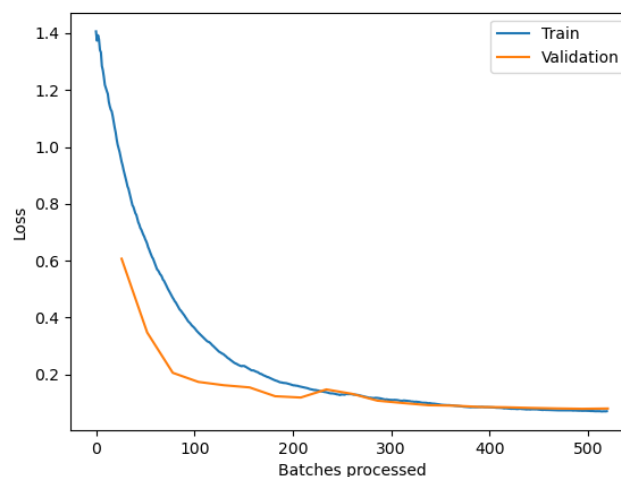


Figure 2. The loss graph of the initial U-net model.

Per class metrics:

	NoData	water	vegetation	built area	bare ground
precision	0	0.958128	0.931627	0.943199	0.918898
recall	0	0.990565	0.739906	0.956589	0.901517
f1	0	0.974077	0.824771	0.949847	0.910125

Table 1. Metrics for each LULC class of the initial U-net model.

Building upon the foundation from the initial model, transfer learning was employed to refine the model. This approach refined the classification capabilities of the deep learning model and provided a significant improvement in accuracy and loss minimization. As illustrated in Figure 3, the second model shows a smoother convergence pattern compared to the initial model. The training loss consistently decreased over epochs, reaching

approximately 0.10 by the final epoch, and validation loss stabilized at around 0.12. This behavior indicates that the model effectively generalized during the training process, with limited overfitting issues. It should be noted that fluctuations observed in the validation loss were attributed to the heterogeneity of the dataset and the complexity of class boundaries. However, the overall low loss values provided a strong indication of effective learning. These fluctuations did not hinder the model's ability to generalize effectively.

The refined model also demonstrated substantial improvements, particularly for vegetation, with an F1-score of 0.86, along with precision and recall values of 0.89 and 0.83, respectively (Table 2). All other classes maintained or improved their metrics compared to the initial model. This enhanced performance validated the effectiveness of transfer learning in addressing class-specific challenges and achieving more accurate LULC classification.

Figure 4 presents a visual comparison between the classification results and the raw PlanetScope imagery for April 14 (pre-rainfall), April 18th (one day post-rainfall), and April 20th (three days post-rainfall) for a zoom-in part of the study area. The pre-rainfall classified image demonstrates the model's ability to delineate water, vegetation, built areas, and bare ground with clear boundaries. These results align well with the corresponding raw imagery, demonstrating the model's robustness in detecting subtle spectral variations.

The classification results demonstrate the advantage of high-resolution PlanetScope imagery for capturing fine-scale LULC patterns, particularly in complex urban environments where conventional 10-meter resolution Sentinel-2 data may lack sufficient detail. The use of 3-meter PlanetScope imagery allowed for the detection of small vegetation patches, narrow water bodies, and small built structures, which are often misclassified in coarser-resolution imagery.

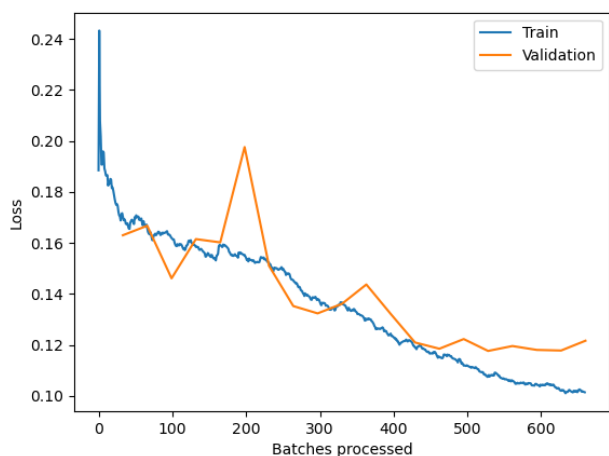


Figure 3. The loss graph of the refined U-net model trained from the initial model via transfer learning.

Per class metrics:

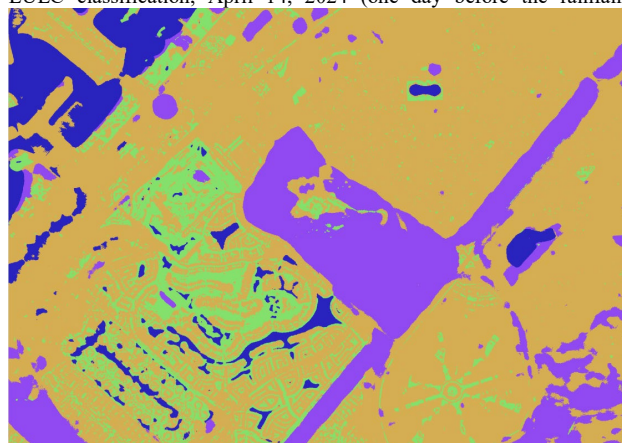
	NoData	water	vegetation	built area	bare ground
precision	0	0.979104	0.890033	0.958372	0.921921
recall	0	0.983488	0.829735	0.961130	0.921260
f1	0	0.981291	0.858827	0.959749	0.921590

Table 2. Metrics for each LULC class of the refined U-net model.

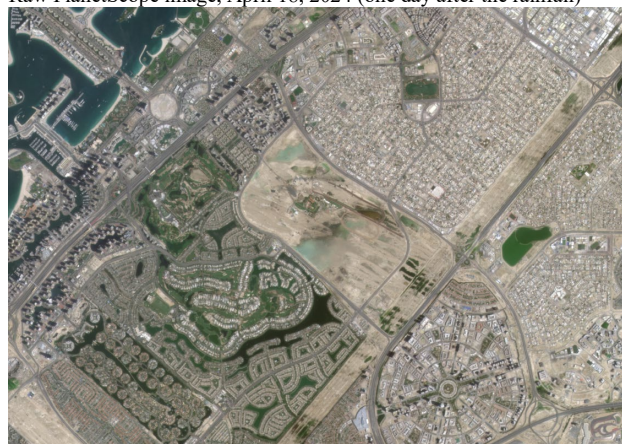
Raw PlanetScope image, April 14, 2024 (one day before the rainfall)



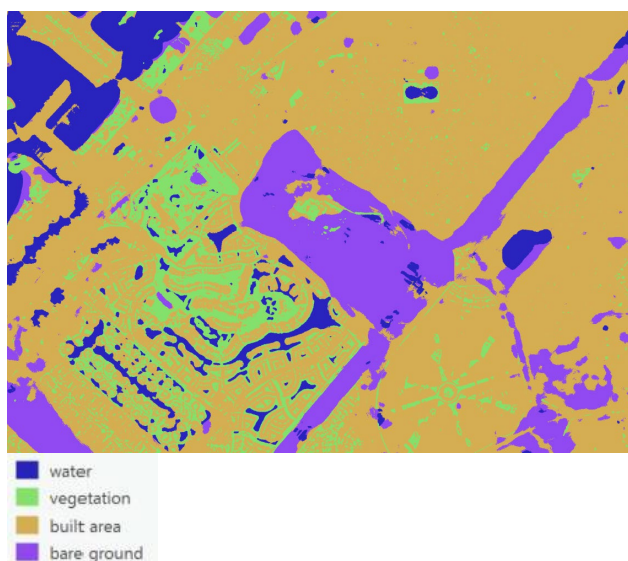
LULC classification, April 14, 2024 (one day before the rainfall)



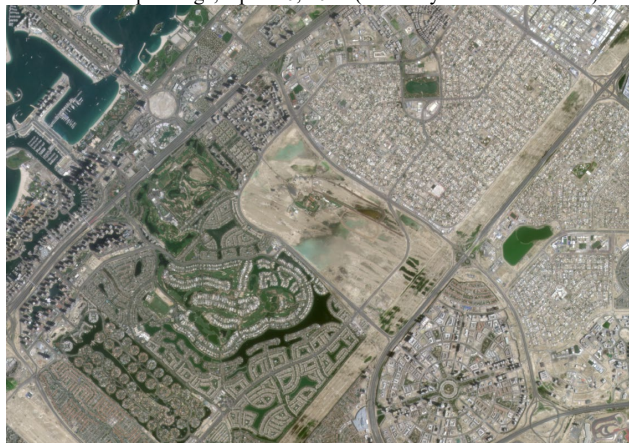
Raw PlanetScope image, April 18, 2024 (one day after the rainfall)



LULC classification, April 18, 2024 (one day after the rainfall)



Raw PlanetScope image, April 20, 2024 (three days after the rainfall)



LULC classification, April 20, 2024 (three days after the rainfall)

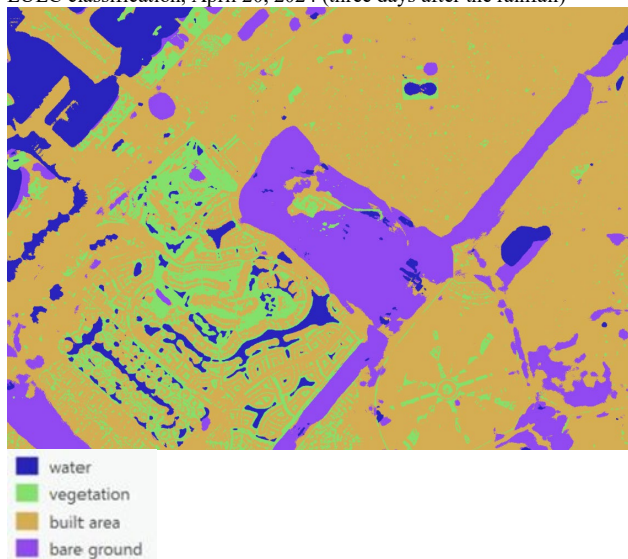


Figure 4. Visual comparison of the classification results and the raw PlanetScope images before and immediately after the rainfall.

3.2 Flooded Areas and Post-Rainfall Recovery Patterns

Flooded areas were identified by analyzing LULC changes from vegetation, built area, and bare ground to water during the period between April 14 (pre-rainfall) and April 18 (post-rainfall). As illustrated in Figure 5, the flooded areas were distributed across Dubai, with larger zones observed in the Ras Al Khor Wildlife Sanctuary near Dubai Creek, the coastal World Islands, and industrial areas such as National Industries Park and Dubai Industrial City in the south. These flood-affected zones are further summarized in descriptive statistics shown in Figure 6. In total, approximately 23.8 km² of the areas were flooded. Among them, bare ground accounted for the largest share at 15.65 km² (66 % of the total affected area). Built area comprised 7.65 km² (32 %), while vegetation was 0.49 km² (2 %). These findings suggest that bare ground and built area were the most vulnerable landscapes to flood events, while vegetation demonstrated greater resilience to floodwaters. The lower flood susceptibility of vegetation could be attributed to higher soil infiltration and vegetative barriers reducing direct water accumulation.

The flooded areas, as illustrated in Figures 5 and 6, were subsequently monitored for recovery from water to non-water classes on different post-rainfall dates (Figure 7). On April 20th, three days after the rain, most flooded areas remained waterlogged, which accounted for 22.5 km² or 95% of the total flooded area. This persistence of standing water highlights the slow drainage process and poor permeability in urban areas.

By April 25th, eight days after the rainfall, there was a significant decrease in water-covered areas, from 22.5 km² to 12.85 km². This 43% reduction in water extents indicates partial recovery primarily in built areas and bare ground, which suggests that floodwaters drained may be more effectively in some urbanized regions with stormwater management infrastructure.

By April 27th, ten days after the rain, 8.8 km² of the flooded areas (37% of the initially flooded land) were still unrecovered, despite 6.1 km² of built area and 8.5 km² of bare ground had fully recovered. The slow recovery in certain areas highlights the persistent flood risks in urban and industrial zones. In addition, no significant differences were observed in the recovery rates between built areas and bare ground, which suggests that both LULC types were equally susceptible to flooding and required similar recovery times. Future research should focus on spatiotemporal flood dynamics over extended post-event periods. Perhaps, hydrological modeling and field validation can be included to further analyze the persistence of floodwaters in different LULC classes.

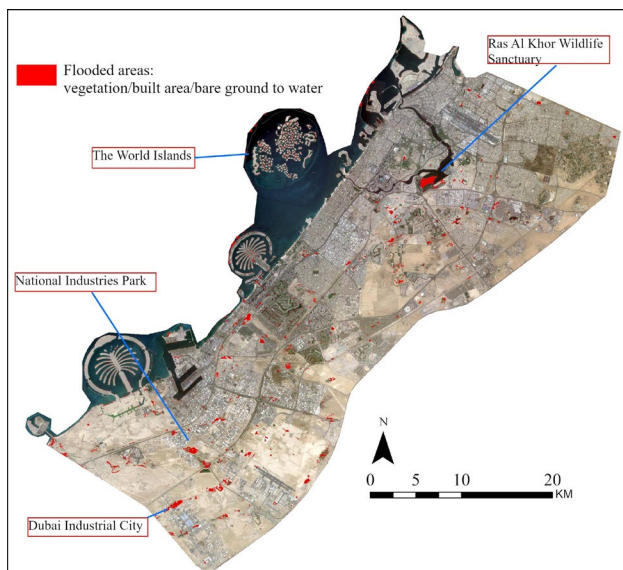


Figure 5. The flooded areas due to the April 14-17 rainfall.

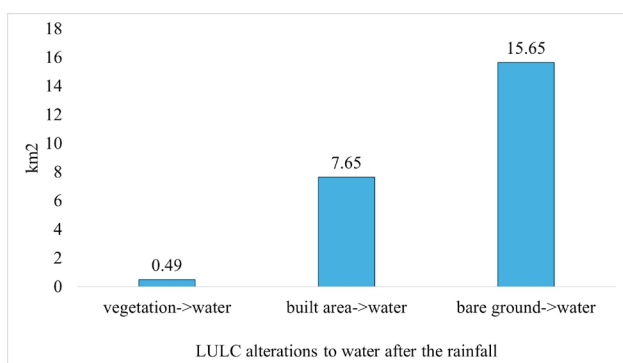


Figure 6. The flooded areas on April 18, immediately after the rainfall.

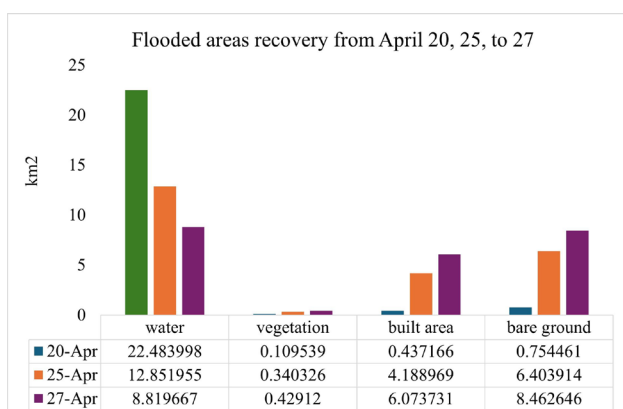


Figure 7. Flooded areas recovery from April 20 (3 days after the rainfall), April 25 (8 days after), to April 27 (10 days after).

4. Conclusion

This study assessed the impact of the April 2024 extreme rainfall event in Dubai using high-resolution PlanetScope imagery and a U-Net deep learning model for LULC classification. By integrating Sentinel-2-derived LULC data to refine the sample dataset, a U-Net model with high classification accuracy was achieved through transfer learning. The trained model was

applied to map pre- and post-rainfall LULC distributions and assist in identifying flooded areas. Flood-induced land cover changes and post-rainfall recovery of different LULC categories were also detected and analyzed in a GIS environment.

The results revealed that approximately 23.8 km² of land was flooded, which is equivalent to about 10 times the area of Downtown Dubai. Among the flooded areas, bare ground (66%) and built-up areas (32%) are the most affected landscapes, while vegetation (2%) showed greater resilience to floodwaters. Post-rainfall recovery monitoring showed that floodwaters persisted for several days, with 95% of flooded areas still submerged three days after the rain. By April 25, water coverage decreased by 43%, indicating partial recovery, predominantly in built-up areas and bare ground. However, 37% of the initially flooded area remained underwater even after ten days, which suggests a slow recovery process across urban landscapes. These results indicate that while Dubai's built infrastructure exhibited a moderate recovery rate, large portions of the affected land remained inundated for extended periods.

This research demonstrates the effectiveness integrating high-resolution remote sensing and deep learning for urban flood impact assessment. The study highlights the advantages of PlanetScope imagery in capturing fine-scale post-disaster changes and validates the use of transfer learning to improve LULC classification accuracy, particularly for vegetation. However, this research can be strengthened by including more training data for minority classes, particularly from post-rainfall scenes. Robust performance metrics and clear visual validations would further improve the model's reliability. Future studies should also explore spatiotemporal LULC change dynamics over longer periods and investigate how flooding affects different urban and natural landscapes over time.

Acknowledgements

This study was funded by the Zayed University Start-Up Grant for the research period from December 2023 to June 2025. The grant code is 23022.

References

- Ahmad, R., Tondo, L., Holmes, O. 2024. "Desert city of Dubai floods as heaviest rainfall in 75 years hits UAE". *The Guardian*. <https://www.theguardian.com/world/2024/apr/17/dubai-floods-uae-rainfall-weather-forecast> (9 February 2025)
- Alawlaqi, A. W. 2024. "'We underestimated this storm': UAE residents face electricity, water outages after flooding, heavy rains". *Khaleej Times*. <https://www.khaleejtimes.com/uae/we-underestimated-this-storm-uae-residents-face-electricity-water-outages-after-flooding-heavy> (3 January 2025)
- Basheer, S., Wang, X., Nawaz, R. A., Pang, T., Adekanmbi, T., Mahmood, M. Q. 2024. A comparative analysis of PlanetScope 4-band and 8-band imageries for land use land cover classification. *Geomatica*, 76(2), 100023. <https://doi.org/10.1016/j.geomat.2024.100023>
- Chanda, M., Hossain, A. K. M. A. (2024). Application of planetscope imagery for flood mapping: a case study in South Chickamauga Creek, Chattanooga, Tennessee. *Remote Sensing*, 16(23), Article 23. <https://doi.org/10.3390/rs16234437>

Cornish, C., Georgiadis, P. 2024. "Dubai airport struggles for third day amid travel chaos after storm". *Financial Times*. (10 May 2024)

ESRI. 2024. "United Arab Emirates Region Boundaries". <https://www.arcgis.com/home/item.html?id=6b25e7dfef5445878fdcd4579c143fd0> (10 May 2024)

JBA Event Response. 2024. "Dubai Floods: April 2024". *JBA Risk Management*. <https://www.jbarisk.com/knowledge-hub/event-response/dubai-floods-april-2024/> (12 December 2024)

Lombana, L., Martínez-Graña, A. 2022. A flood mapping method for land use management in small-size water bodies: validation of spectral indexes and a machine learning technique. *Agronomy*, 12(6), Article 6. <https://doi.org/10.3390/agronomy12061280>

McCabe, K. 2024. "Dubai floods and cloud seeding". *Royal Meteorological Society*. <https://www.rmets.org/metmatters/dubai-floods-and-cloud-seeding> (10 May 2024)

Oxford Analytica. 2024. Flash floods will increase in frequency in the Gulf. <https://doi.org/10.1108/OXAN-DB286682> (10 May 2024)

Planet. 2025. *Education and Research Program*. <https://www.planet.com/industries/education-and-research/>

Planet Labs PBC. 2024. "Planet Application Program Interface: In Space for Life on Earth". <https://api.planet.com> (10 May 2024)

Rannard, G. 2024. "Deadly Dubai floods made worse by climate change". *BBC News*. <https://www.bbc.com/news/science-environment-68897443> (10 May 2024)

Redlands, ESRI. 2025. ArcGIS Pro Software, Version 3.4.

Ronneberger, O., Fischer, P., Brox, T. 2015. U-Net: convolutional networks for biomedical image segmentation. In N. Navab, J. Hornegger, W. M. Wells, A. F. Frangi (Eds.), *Medical Image Computing and Computer-Assisted Intervention – MICCAI 2015* (pp. 234–241). Springer International Publishing. https://doi.org/10.1007/978-3-319-24574-4_28

The National. 2024. *Emirati dies in flash floods as record rainfall lashes UAE*. <https://www.thenationalnews.com/news/uae/2024/04/17/emirati-dies-in-flash-floods-as-record-rainfall-lashes-uae/> (9 February 2025)

UAE GOV [@UAEmediaoffice]. 2024. <https://t.co/lir6ZS2Dzs> [Tweet]. *Twitter*. <https://x.com/UAEmediaoffice/status/1780326720588906951> (10 May 2024)